Petrology, Vol. 7, No. 1, 1999, pp. 91–101. Translated from Petrologiya, Vol. 7, No. 1, 1999, pp. 99–110.

Convection and Redistribution of Alkalis and Trace Elements during the Mingling of Basaltic and Rhyolite Melts

I. N. Bindeman and A.M. Davis

Department of Geophysical Sciences and the Enrico Fermi Institute, University of Chicago, S. Ellis ave. 5734, Chicago, IL 60637 U.S.A. e-mail: inbindem@midway.uchicago.edu

Received May 20, 1998

Abstract—Numerous examples of long-lasting coexistence of basaltic and rhyolitic magmas in magma chambers indicate that it results in thermal, isotopic, and chemical exchange between the melts. This paper presents our model experiments, which demonstrate the effect of rapid potassium and sodium diffusion from the basaltic to rhyolitic melt on their density and resultant convection in each of the melts. This diffusion-induced convection leads to the rapid preferential redistribution of alkalis between the melts. Ion microprobe profiles demonstrate that rapidly diffusing trace elements are transported more quickly than bi-, tri-, and tetravalent major components, and, at the very beginning of the experiments, they were redistributed between the melt in correspondence with respective partition coefficients typical of these components when the acid and mafic melts are immiscible. Convection maintains significant chemical gradients and creates a self-sufficient mechanism for the convection, diffusion, and redistribution of trace elements and alkalis between the magmas.

INTRODUCTION

The coefficients of chemical diffusion of network-modifying elements (CaO, MgO, and FeO) are roughly commensurable with one another and with the coefficients of network-forming elements (SiO_2 and Al_2O_3) (Liang *et al*., 1996; Kress and Ghiorso, 1993). This is caused by the strong coupling between diffusing components, i.e., a dependence of the diffusion coefficient of each component not only on its own concentration gradient but also on the concentrations and concentration gradients of all other components. Contrary to them, the diffusion of isotopes (self-diffusion) is independent of the gradients of other components, and, thus, the redistribution of isotopes between magmas can proceed one–two orders of magnitude faster than chemical mixing (Lesher, 1994; Perez and Dunn, 1996). Many trace elements are characterized by high values of diffusion coefficients (Lesher, 1994; Baker, 1992; Hofmann, 1980), because, contained in low concentrations, these elements are less dependent on the gradients of major components. Alkalis (K_2O and Na_2O) are also able to diffuse several times faster than network modifiers and formers (Watson and Baker, 1991; Baker, 1992). This process often proceeds in the direction opposite to the gradient of alkali concentrations and is coupled with uphill diffusion (Watson and Baker, 1991; Bindeman and Perchuk, 1993).

Since the transport of trace elements and alkalis between magmas can proceed faster than the mixing of major components, this can serve as an efficient mechanism of their rapid redistribution between the melts. However, diffusion is a slow process, which cannot ensure a large-scale redistribution. Thermally or compositionally driven convection in each of the coupled magmas (Litvinovsky and Podladchikov, 1993) can facilitate this transfer through sustaining strong diffusion gradients at the interface between the magmas.

The aim of our study is to demonstrate the results of ion microprobe examination of the products of experimentally modeled mixing between basalt and rhyolite. These results indicate that the rapid diffusion of alkalis in magmas is sufficient to stimulate and maintain compositional convection in them. This is caused by the high partial volumes of K_2O and Na_2O (Lange and Carmichael, 1990) and the resultant permanent instability of the system. Convection of this type leads to the rapid redistribution of many trace elements between magmas and provides a model mechanism for mixing in magmatic chambers.

EXPERIMENTAL GOALS

We conducted a series of experiments on magma mixing using a cylinder–piston apparatus with large graphite capsules and assemblies of soft ceramics with heaters tapered in the margins to minimize the temperature gradient within the assembly. The large tallness and diameter of the assemblies (10 by 4 mm) and, hence, their large volumes and the high experimental temperatures allowed us to create conditions for modeling compositional convection in the course of the mixing of rhyolite and basalt melts. The conventional experimental procedures (with lower temperatures and, consequently, a higher viscosity of the melt, and with assemblies of smaller volume) do not allow convection to be observed (Watson and Baker, 1991; Lesher, 1994; etc.).

Chemical composition and physical properties of starting materials

Oxide	Rhyolite		Basalt	
SiO_2	75.09	*Ap* 0.23	48.96	*Ap* 0.21
TiO_2	0.36	*Ilm* 0.71	0.80	*Ilm* 1.47
Al_2O_3	12.48	*Or* 6.43	15.50	*Or* 10.00
FeO	3.28	*Ab* 40.36	9.52	*Ab* 12.93
MnO	0.10	*An* 10.68	0.20	*An* 17.67
MgO	0.44	*Di* 1.20	9.33	*Di* 23.88
CaO	2.50	*Opx* 2.67	9.65	*Opx* 0.00
Na_2O	4.60	*Qtz* 37.72	4.20	*Qtz* 11.61
K_2O	1.05		1.75	
P_2O_5	0.10		0.10	
Total	100		100	
Diffusion coefficients (Watson and Baker, 1991; Hofmann, 1980)				
D_K, cm^2/s	$10^{-6.5}$		10^{-6}	
D_{Na}, cm^2/s	$10^{-5.5}$		$10^{-5.3}$	
Melt density (Lange and Carmichael, 1990)				
ρ, g/cm^3	2.63		2.90	
Kinematic viscosity (Bottinga and Weill, 1972)				
ν, cm^2/s, melts	3.5×10^3		10	
ν, cm^2/s, boundary layers δ	2×10^3		20	

In a separate series of experiments, we paid particular attention to the redistribution of alkalis between the acid and mafic magmas of various alkalinity and to the effect of this phenomenon on the overall density of contacting melts. Some experiments were conducted in an attempt to model compositional convection that would reproduce a geologically realistic situation of a basaltic magma layer underplating a layer of acid melt.

A potassium and sodium flux from the basalt to rhyolite melt can be realized through the uphill diffusion mechanism: although rhyolite is usually higher in alkalis than basalt, the activity coefficients of alkalis are 1.5–2 times higher in basaltic than in rhyolitic melt (Bindeman and Perchuk, 1993). This means that, at initially equal contents of both alkalis, uphill diffusion (opposed to the concentration gradients) of these elements will occur in the contacting melts, and elements will start to redistribute from the mafic to the more acid melt.

Component redistribution between silicate melts can result in density variations caused by the different mole volumes of diffusing components (Liang *et al.*, 1996). Alkalis have the largest mole volumes among major components (Lange and Carmichael, 1990), and their redistribution within or between magmas should supposedly result in the largest density changes, which are favorable for compositional convection.

However, in most experiments described in the literature, rapid potassium diffusion is often counterbalanced by sodium diffusion in the opposite direction (Watson and Baker, 1991), and this process either offsets or strongly reduces the effect of density changes. Our experiments were deliberately conducted in a manner to ensure the uphill diffusion of both sodium and potassium from the basaltic to rhyolitic melt. We added 1.5 wt % potassium and sodium to the initial tholeiitic melt to create approximately equal concentrations of alkalis in the coupled melts (Fig. 1) at the higher activities of these elements in the basaltic liquid. The resultant basalt became nepheline-normative, resembling typical alkali basalt.

EXPERIMENTAL AND ANALYTICAL PROCEDURES

Our experiments were carried out at a cylinder–piston apparatus at the Institute of Experimental Mineralogy, Russian Academy of Sciences, (Bindeman and Perchuk, 1993) and the Laboratory of High Pressures, University of Chicago, at 1450°C and 12 kbar. We used large graphite capsules 1 cm high, with an inner diameter of 4 mm. The capsules were placed into large assemblies of soft ceramics 2 in. high and 3/4 in. in diameter, which were manufactured of the materials and from drawings provided by courtesy of I. Kushiro (1976). The graphite heaters in the assemblies were ground off in the margins at an angle of ~3° to enlarge both the usable volume of the assembly and the zone with the minimum temperature gradient (10–20°C) within an assembly up to 1 cm (Kushiro, 1976). Graphite capsules were used to prevent iron loss and sustain most of it in the form of FeO (Thompson and Kushiro, 1972; Holloway *et al.*, 1992). The starting materials were natural vitreous basalt and rhyolite from Kunashir Island, Kuril Islands. The rhyolite glass and basaltic glass with added 1.5 wt % K_2O and Na_2O (in the form of K_2CO_3 and Na_2CO_3) were preliminarily remelted for 1.5 h under the conditions of the experiments. The composition of the glasses was analyzed on an electron microprobe (table). Before the experiment, the natural basalt was fused and, on quenching, powdered under acetone. The basaltic glass thus prepared was placed at the bottom part of the capsule, pressurized, and covered with a layer of rhyolitic glass. The material was heated and brought to the desired pressure for less than 10 min. The quenching was practically instantaneous and achieved by means of switching off the current at continuing water cooling.

The experimental products were used to prepare polished thin sections, which were examined by a variety of methods. The contents of major elements were determined and X-ray compositional maps were obtained on a Cameca SX-50 microprobe at the University of Chicago. Trace elements were analyzed on a modified AEI IMS-20 ion microprobe at the same university. Details of the technique of glass analysis on an

(a)

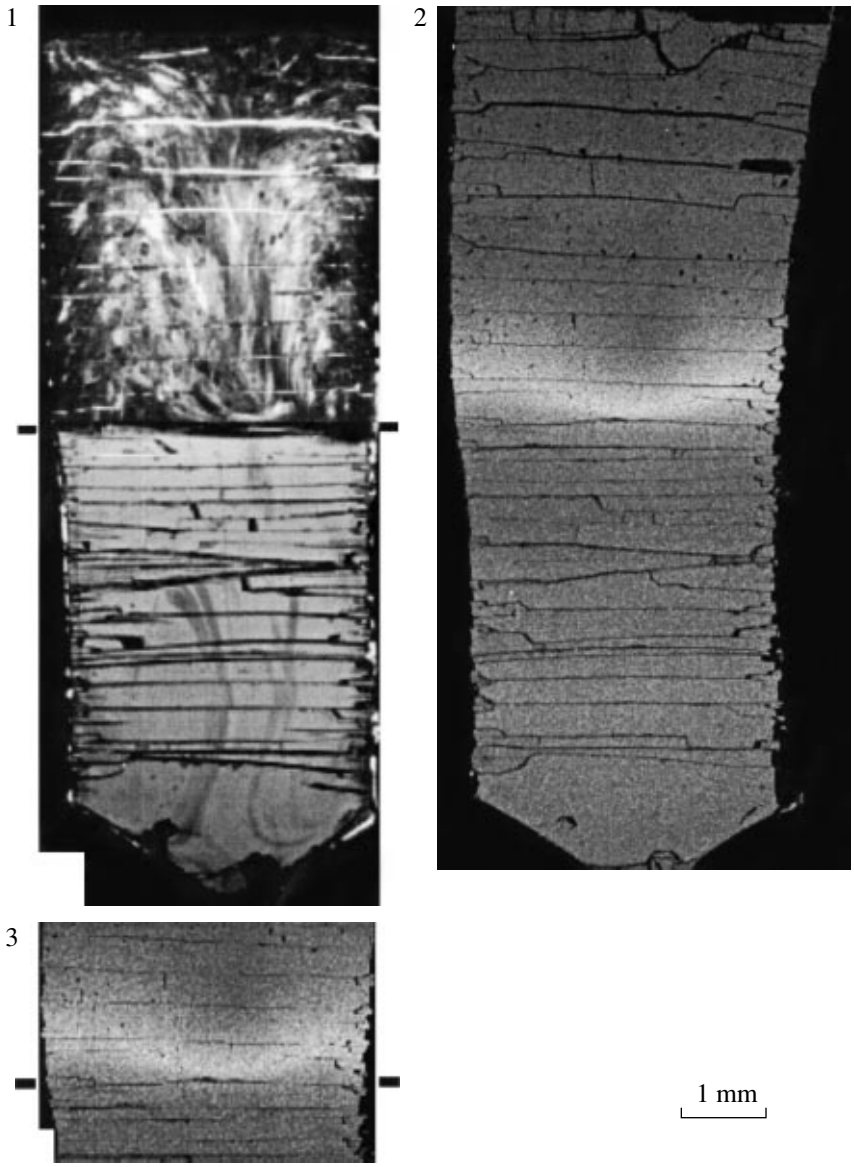

Fig. 1. Convection during the mixing of basaltic and rhyolitic melts.

(a) (1) Optical microphotograph of a thin section of Run BR-7 products showing "quenched" convective textures in coupled basaltic (bottom) and rhyolitic (top) melts. Tiny graphite particles accentuate the convective texture. (2) Back-scattered electron image showing the distribution of K. (3) Enlarged fragment of the previous figure (two horizontal marks at the figure sides indicate the boundary between the melts).

(b) Topochemical maps showing the distribution of major elements that accentuate convective textures and convection-controlled redistribution (see text for discussion).

ion microprobe are given in (MacPherson and Davis, 1993; Bindeman *et al*., 1998). The contents of CO_2 and H_2O were analyzed on a Nicolet NMR IR spectrometer in a doubly polished platelet that was prepared of the products of experiment BR-7.

RESULTS

Three thin sections made of the products of 3-h-long experiments contain quench textures, which can be interpreted as convection flows "quenched" in the basaltic and rhyolitic glasses.

X-ray mapping of the whole thin-section area (accomplished on a microprobe) provides evidence of the apparent uphill diffusion of both alkalis from the basalt toward rhyolite, as can be inferred from the enrichment of these elements in the lower portion of the rhyolitic glass layer and their depletion in the upper basaltic glass layer (Figs. 1a–1b). The uphill diffusion

(b)

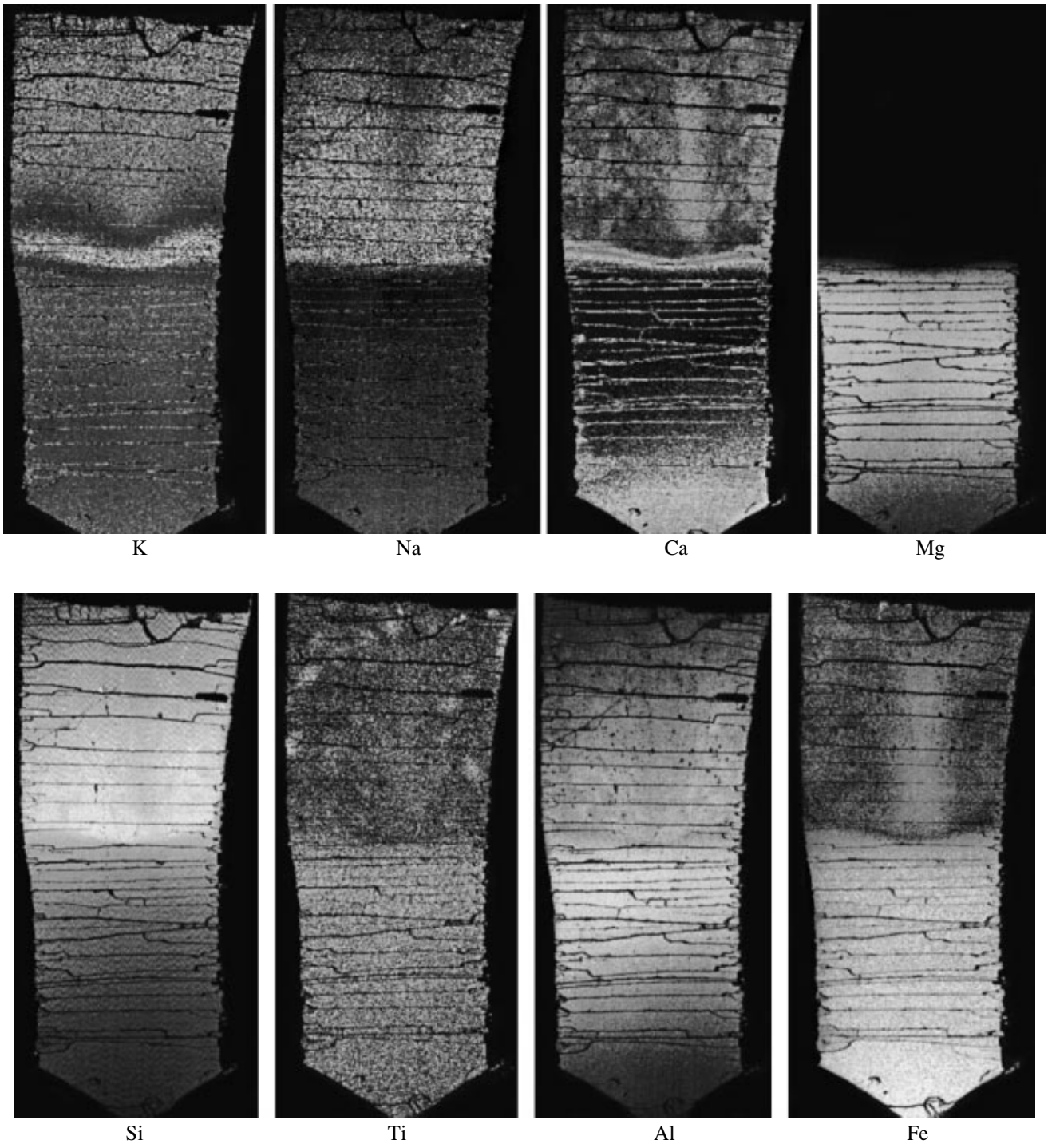

Fig. 1. (Contd.).

profiles of both of the alkalis are also seen in the compositional profile across the ampoule (Fig. 2a). The results of a detailed study of the most representative run BR-7 will be presented below.

Optical photomicrographs demonstrate two convective cells, which are marked with tiny graphite particles in the quenched basaltic glass in the lower portion of the ampoule (Fig. 1a). U-shaped quench "diapiric" textures can be seen in the rhyolitic glass, in which convection seems to have been more intense, although this can be inferred only from the higher content of graphite particles in the glass. Two dynamic boundary zones are

seen on both sides of the boundary between the melts. The total thickness of these layers is equal to the distance between the peaks of alkali uphill diffusion in the compositional profile (Fig. 2a). The convective transfer of matter seems to have been more active at the center of the ampoule, where the thickness of both boundary zones increases threefold (Fig. 1).

Figure 1b demonstrates the redistribution of K_2O, Na_2O, FeO, CaO, and MgO not only along the direction of diffusion but also perpendicular to it in correspondence with the lines of quenched convection flows in the optical microphotograph (Fig. 1a-1). The two descending plumes at the center of the basaltic layer and one plume ascending along the ampoule walls in the rhyolitic layer resulted in an U-shaped bend in the original boundary plane between the melts (Figs. 1a-2 and 1a-3). Note that the U-shaped transfer of excess K_2O and Na_2O along the ampoule walls in the rhyolite is counterbalanced by CaO, FeO, and MgO flows (the latter is pronounced more poorly) at its center (Fig. 1b). This different behavior of the elements is probably explained by the diffusion of pyroxene and feldspar clusters.

A microprobe profile across the ampoule demonstrates that the contents of all major elements changed even at the ampoule walls. Diffusion cannot ensure matter transfer for a distance of 5 mm over an experiment time as short as 3 h at the known diffusion coefficients of major components under the conditions of the experiments (Liang *et al.*, 1996; Kress and Ghiorso, 1993; Watson and Baker, 1991). This transport can be maintained only by convection.

Clearly pronounced potassium and sodium concentration peaks (Fig. 2a) occur in the lower part of the rhyolitic melt, presumably within its dynamic boundary zone. A trough in the potassium content was detected on the other side of the boundary, in the upper portion of the basaltic melt layer. As a result, the rhyolitic boundary zone gained 1.8 wt % K_2O and 1 wt % Na_2O, and this resulted in deficiencies of other principal network-modifying components. Al_2O_3, FeO, CaO, and TiO_2 are depleted in the rhyolitic boundary zone by 1.0, 0.6, 0.4, and 0.1 wt %, respectively. SiO_2, a network forming component, does not comply with this regularity and forms a simple thin mixing zone. H_2O and CO_2, which were analyzed by infrared spectroscopy at their contents of 0.01–0.05 wt %, exhibit the largest mixing zone. Their concentrations correspond to the condition of strong undersaturation with respect to H_2O and CO_2 in the graphite stability field (Thompson and Kushiro, 1972; Holloway *et al.*, 1994).

CAUSES OF CONVECTION

Alkalis have the largest molar volumes among all major components (Lange and Carmichael, 1990). Their enrichment in the diffusion boundary zone of the rhyolitic melt caused by the rapid uphill diffusion of Na_2O and K_2O supposedly leads to the gradual increase in the density-controlled instability (the Rayleigh–Taylor instability). The diffusion of alkalis from the upper part of the basaltic melt also results in an unstable diffusion boundary zone. In order to demonstrate this process, we used a compositional profile across the ampoule (Fig. 2a) and calculated the density at any point at the actual experimental conditions (T = 1450°C, P = 12 kbar; Fig. 2b) with the technique proposed by Lange and Carmichael (1990).

Our calculations indicate that the rhyolite retains a quenched density buoyancy gradient of 0.03–0.04 g/cm^3 throughout the rhyolitic glass layer (compare the densities at the boundary between the melts and that at the ampoule top), and this is directly correlated with the amount of alkalis added. The relative density gradient, $\Delta\rho/\rho$, is equal to 1–2%. It is interesting that the most buoyant portion of the rhyolitic melt occurs in the region with the maximum contents of alkalis. In the basaltic layer, in which convection was more vigorous because of its lower viscosity, the "quenched" density gradient is within the error of analysis and density calculation (~0.005–0.01 g/cm^3).

No convection textures developed in analogous experiments (Bindeman and Perchuk, 1993) with the same rhyolitic and basaltic glasses to which no alkalis were added.

It seems that no convection can be caused by the temperature gradient in the capsules. Even if the gradient within each of the halves of the 1-cm ampoule was supposedly 20–50°C (the temperature was higher at the center and lower near the walls of the ampoule), the thermal Rayleigh number (Ra), which was calculated following the procedure of Bottinga and Weill (1972) for a rhyolitic melt layer with a density as shown in the table, was no greater than one. This is three orders of magnitude lower than its critical values (10^3) needed for convection to begin. Moreover, the thermal gradient of the piston–cylinder assemblies should stabilize the thermal density structure of the basaltic melt layer, because the temperature decreases (and, correspondingly, the density increases) toward the lower end of the ampoule, and, thus, thermal convection cannot occur in the basalt. This provides further support to the concept that this convection is of purely compositional nature and results from the rapid diffusion of alkalis.

The possibility of composition-controlled convection in coupled rhyolitic and basaltic melts is probably determined by the critical thickness of the diffusion boundary layer (δ), which is either enriched or depleted in alkalis (in the rhyolitic and basaltic melts, respectively). As a result, the rhyolitic boundary layer becomes lighter than the overlying rhyolitic melt, and, conversely, the basaltic layer becomes heavier than the underlying basaltic melt. For example, convection begins in the rhyolitic melt layer in response to the growth of the buoyant boundary layer (enriched in alkalis in its lower part) with time. This buoyant diffu-

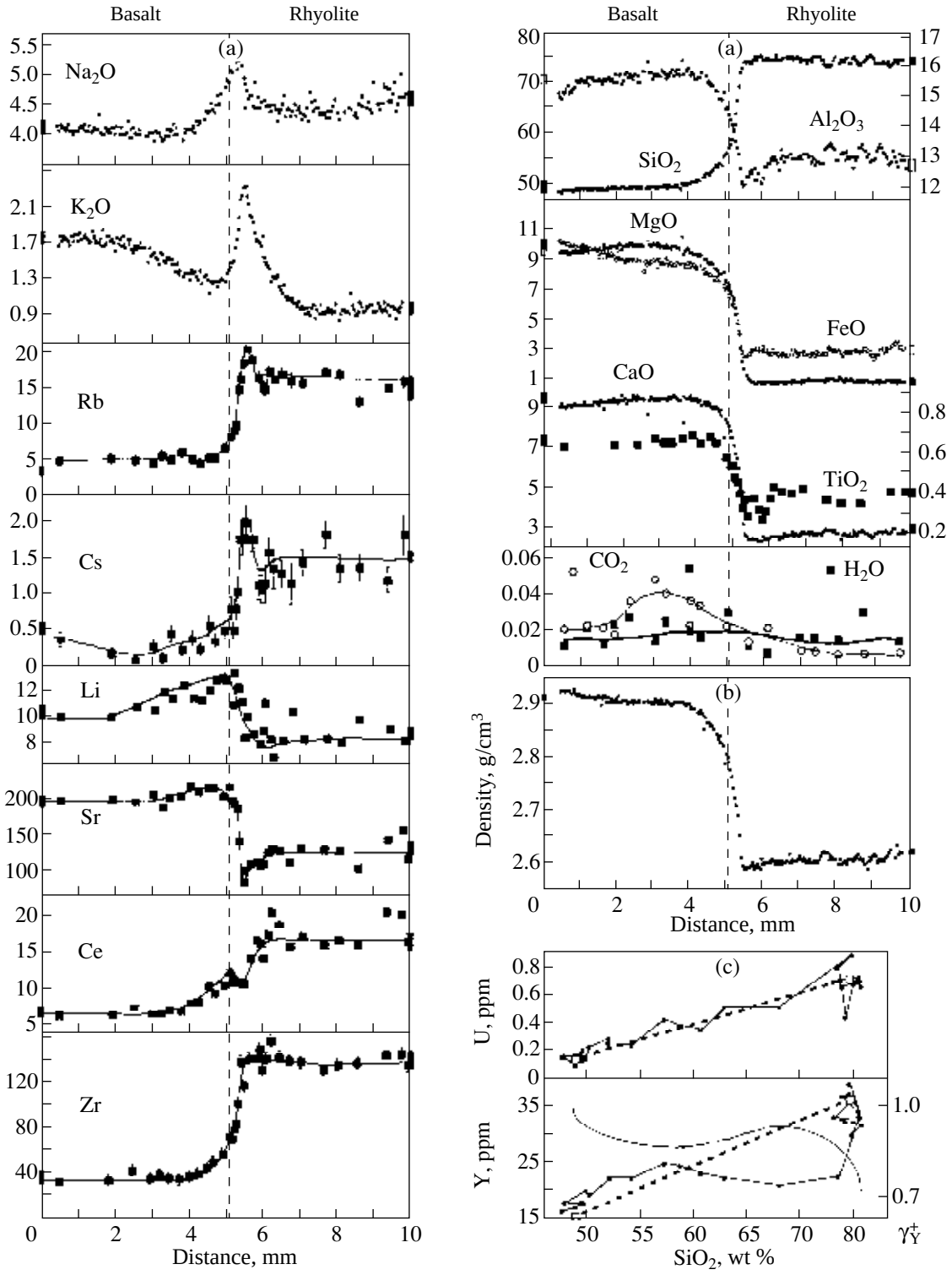

Fig. 2. Behavior of major (wt) and trace (ppm) elements during the mixing of basaltic and rhyolitic melts.

(a) Electron and ion microprobe profiles through the glasses of Run BR-7. The thicknesses of the major-element and Zr mixing zones are similar. Note the uphill-diffusion profile for K_2O, Na_2O, Cs, Rb, Li, Sr, Ce, TiO_2. The dashed line marks the zone of the equal diffusion-controlled transfer of SiO_2. The Z-shaped configuration of the profile for Ce is valid; similar configurations are typical of the profiles for other REEs and Y.

(b) "Quenched" density profile through the capsule, calculated at run conditions (Lange and Carmichael, 1990). Note that a transient negative density gradient is preserved in the rhyolitic glass.

(c) Binary Y–SiO_2 and U–SiO_2 plots showing that the diffusion of Y is faster than that of Si, and the diffusion mobility of U and SiO_2 is similar.

sion boundary zone ($\Delta\rho/\rho$ = 0.01–0.02) will increase proportionally to $x = (Dt)^{1/2}$ at the physical parameters listed in the table. Inasmuch as convection starts at Ra = 10^3, the diffusion layer thickness, δ, at the instant of convection onset, t, can be expressed (Cristensen, 1984) as

$$\delta = 10 \cdot \sqrt[3]{\frac{D \cdot \nu}{(\Delta\rho/\rho) \cdot g}}, \quad (1)$$

where g = 980 cm/s^2, and D is the diffusion coefficient of the density-controlled instability, which can be approximated through the diffusion coefficients for K and Na (table). In the rhyolitic melt, δ will be equal to 1 mm in $t = 10^3$–10^4 s (0.5–2.5 h) after the beginning of the 3-h experiment, i.e., closer to its end. Analogous estimates can be made for the critical thickness of the density-unstable boundary zone in the basaltic melt (~0.1 mm) and the timing of convection onset ($t = 10^2$–10^3 s). These values indicate that convection began nearly immediately after the loss of alkalis from the upper basaltic melt layer due to their diffusion to the rhyolitic melt. The calculated compositional Rayleigh number is 100 times larger in the basaltic melt layer than in the rhyolitic one, and this fact is reflected in the occurrence of two convective cells in the basalt and only one in the rhyolite (Fig. 1a). Conceivably, this early convection in the basalt enhanced the diffusion gradients at the interface between the two melts, and this led to the more active and rapid diffusion of alkalis and their more rapid enrichment in the rhyolitic layer than it would be caused by a purely diffusion-controlled process.

GRADIENTS OF TRACE ELEMENTS

The contents of 39 trace elements in profiles along the ampoule were determined by ion microprobe in the products of two experiments. The concentration profiles of both of them are similar. Figure 2 presents the results of run BR-7.

As can be seen in Fig. 2, the thicknesses of the mixing zones of distinct elements are notably different. Small low-charge ions, such as Li^+, form broad mixing zones, whereas large high-charge ions, as, for example, Zr^{4+}, retain strong gradients, which are commensurable with that of SiO_2.

Although convection changed the original thickness of the diffusion mixing zones, the use of binary element–element plots enables one to reconstruct the relative mobility of elements (Bindeman and Perchuk, 1993). Figure 2c presents an Y–SiO_2 plot with a S-shaped concentration profile, which we interpreted as resultant from the more rapid diffusion of Y than that of SiO_2. At the same time, the linear trend in the U–SiO_2 plot suggests that the diffusion mobility of these components is similar, even if diffusion was disturbed by convection. Analogous diagrams constructed for the rest of the elements revealed the following sequence of their relative mobility:

$$\underset{\text{volatiles}}{(H_2O > Cl > F)} > \underset{\text{alkalis and alkali earths}}{(Li > Na > K \sim Sr > Cs \sim Ba > Rb)}$$

$$> \underset{\text{rare earths}}{(REE \sim Y)} \sim (Ti \sim Pb \sim Sc \sim Mn \sim V)$$

$$> \underset{\text{HFSE}}{(Zr \sim U \sim Th \sim Nb \sim Cr \sim Co \sim Hf \sim P)}$$

$$\sim \underset{\text{major elements}}{(Al_2O_3 \sim MgO \sim CaO \sim FeO)} > \underset{\text{silica}}{SiO_2}$$

This sequence is similar for the basalt and rhyolite. In spite of the nonrigorous character of this procedure, the sequence established above is in good agreement with tracer-diffusion experiments, which demonstrate a decrease in the mobility of elements with the increasing size and charge of the respective ions (Hofmann, 1980; LaTourette *et al.*, 1996; Jambon, 1982). Water and alkalis are characterized by the largest diffusion coefficients, which are one–two orders of magnitude higher than those of the alkali earths. The diffusion coefficients of trivalent REEs and some other trivalent elements are somewhat lower. SiO_2, a network-forming component, has the lowest diffusion coefficient among major elements, and the lowest coefficients among trace elements are typical of U, Th, Nb, Ta, and Zr.

It is pertinent to note that even large and high-charge elements such as REEs diffuse approximately twice faster than SiO_2 (Richter, 1993; Lesher, 1994). The mobility sequence listed above indicates that volatiles, alkalis, and alkali- and rare-earth elements can be exchanged between magmas more quickly than major components, whereas the exchange rates of most HFSEs and transitional elements are similar to those of major elements.

As can be seen in concentration–distance plots, most fast-diffusing trace elements compose uphill and downhill concentration peaks, which resemble those of alkalis (Fig. 2). These peaks are best preserved in the viscous rhyolite, in which convection was not as vigorous and lasted not so long (see above). At the same time, the trace-element concentration gradients between the two peaks are largely situated within the mechanical boundary layers that were not affected by convection. Convection in the interiors of each of the melts facilitated the overall transport of trace elements to the layers.

The fast redistribution of trace elements, K_2O, and Na_2O and the uphill–downhill patterns of their profiles at the boundary between the melts led us to regard the coupled basaltic and rhyolitic melts at the starting moment of their interaction as two magmas actually immiscible with respect to slowly diffusing major elements by exchanging by trace elements and alkalis.

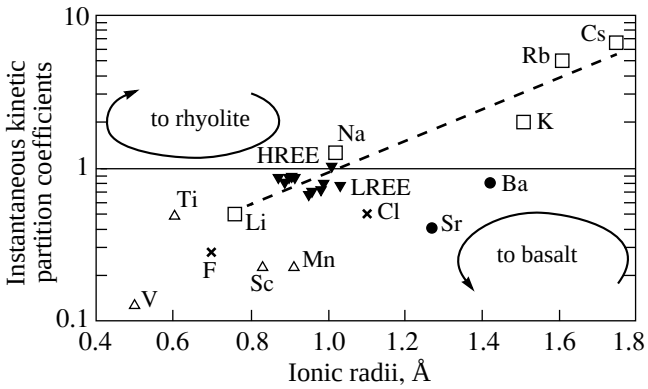

Fig. 3. Instantaneous kinetic partition coefficients (IKPC) for fast-diffusing trace elements (see text).
Note that larger ions within each valence group have larger partition coefficients.

INSTANTANEOUS KINETIC PARTITION COEFFICIENTS

Concentration maxima and minima in the concentration–distance plots can be employed to define the instantaneous kinetic partition coefficients (IKPC) for trace elements and alkalis: these values are the ratios of the peak concentrations in the rhyolitic to those in basaltic glasses (Fig. 3; Bindeman and Davis, 1997). The ratios were calculated for all of the analyzed trace elements for which uphill–downhill profiles were observed in the concentration–distance plot (Fig. 2). The ratios of the peak contents in the rhyolite to analogous contents in the basalt were plotted in a diagram of the type commonly used to illustrate the partition of components between truly immiscible phases (Fig. 3).

Note that the IKPC thus defined for fast-diffusing elements of various valences are in full agreement with equilibrium partition coefficients determined previously for truly immiscible melts (Vicenzi *et al*., 1994; Watson, 1976; Ryerson and Hess, 1978). The IKPC for univalent alkalis cluster along a straight line in an IKPC–ionic radius plot. The small Li ion (IKPC = 0.5) exhibits uphill diffusion from the rhyolitic to basaltic melt, whereas the rest of alkalis with larger ions, particularly Rb and Cs, diffuse uphill into the rhyolitic melt and also show clear-cut maxima and minima with IKPC > 1 for all elements.

Other trace elements exhibit uphill–downhill diffusion patterns and have IKPC < 1. All of them partition from the acid into basaltic melt, with smaller and higher charged ions partitioning more efficiently. This effect was detected in experiments on trace-element partition between truly immiscible melts (Vicenzi *et al*., 1994; Minarik *et al*., 1996; Watson, 1976).

The IKPC for CO_2 is equal to 0.25, which is caused by the higher CO_2 solubility in basaltic than in rhyolitic melt. Carbon dioxide dissolves as the CO_3^{2-} carbonate complex in the former, whereas in the latter, it is dominated by the molecular form (Holloway and Blank, 1994). The IKPC of H_2O is equal to one, a fact suggesting the absence of chemical differences between the H_2O solubility in basaltic and rhyolitic melts, because all H_2O is present as OH^- at its contents of 0.01–0.1 wt % (Holloway and Blank, 1994).

DISCUSSION

IKPC can be employed to predict the ratios of trace-element activity coefficients in coupled rhyolitic (R) and basaltic (B) melts. When using IKPC, we assume that the chemical potentials of fast-diffusing trace elements are equal in the coupled melts

$$\mu_{Rb}^{R} = \mu_{Rb}^{B}. \quad (2)$$

Provided elements occur in the same form in the coupled basalt and rhyolite in our high-temperature superliquidus experiments, then their standard states, μ^0, are the same in both melts. Thermodynamic equilibrium at a constant temperature and pressure requires equal activities of elements, for example, Rb, in the coupled melts

$$a_{Rb}^{R} = a_{Rb}^{B}. \quad (3)$$

Inasmuch as $a_{Rb} = \gamma_{Rb}C_{Rb}$, this leads to a simple relation between the activity coefficients (γ) of a component

$$\text{IKPC} = C_{Rb}^{R}/C_{Rb}^{B} = \gamma_{Rb}^{B}/\gamma_{Rb}^{R}, \quad (4)$$

which makes it possible to determine the activity coefficient of this component in each of the melts, provided its activity coefficient in the other melt is known (Bindeman and Perchuk, 1993).

Numerical simulation of trace-element diffusion by the finite difference method led us to determine (1) how well the IKPC values derived from the profiles of Figs. 2 and 4 fit the actual ratios of activity coefficients and (2) how much faster the diffusion of a trace element should be to result in its redistribution in accordance with equation (4). IKPC can be defined by two parameters: the ratio of the diffusion coefficient of a fast-diffusing trace element to that of a slowly-diffusing major component (for example, SiO_2), D_i/D_{SiO_2}, and the ratio of the activity coefficients of this fast-diffusing trace element, *i*, in each of the melts [see equation (4)] (Zhang, 1993). The simulation also demonstrated that, in the absence of convection, when $D_i/D_{SiO_2} = 2$, IKPC amounts to 70% of its actual value for an infinitely large D_i/D_{SiO_2} ratio. This implies that even the redistribution of slowly-diffusing trace elements ($D_i/D_{SiO_2} \sim 2$), such as REEs (Richter, 1994), approaches relation (4). At the same time, IKPC deviate from the true partition coefficients for true immiscible liquids.

The activity coefficients (γ_i) in melt are a function of the melt composition. This function can be expressed

through the slowly-diffusing major component SiO_2, because the activities of fast-diffusing trace elements are nearly equal within the narrow mixing zone between the uphill and downhill concentration peaks in the diffusion profile (Figs. 2a, 4a, and 4b). If the concentration of SiO_2 is used as a measure of the melt composition, then the S-shaped trajectory between the concentration minimum and maximum of a trace element in binary element–SiO_2 plots (Fig. 4c) can be transformed into γ_i/SiO_2 relation as a mirror image in order to comply with the condition of the constant activity of the trace element between the two peaks [in accordance with equation (3)].

The fast diffusion of trace elements through the interface between the coupled melts implies that convection in the interiors of each of the melts sustains large gradients in the boundary layers and creates favorable conditions for the efficient trace-element redistribution, in accordance with their IKPC, between the magmas.

The linear correlations between the IKPC of alkaline elements and their ionic radii can be explained by the models of acid-base interaction between components in silicate melts (Korzhinskii, 1966). The NBO/T ratio used in the oxygen model (Mysen, 1991) can be employed as a measure of the "acidity–basicity." Stronger bases of all valence groups are redistributed more easily into more acid melt, in which their activity coefficients and NBO/T ratios are lower.[1] At the same time, highly charged smaller ions are prone to form oxide anions, as, for example, YO_3^{3-} and UO_6^{6-}. This process requires larger amounts of nonbridging oxygen (a higher NBO/T ratio), which can be attained in the more basic basaltic melt, and, hence, the activity coefficients of these trace elements in basaltic melt are lower.

Conversely, the redistribution of strong bases, such as Na, K, Rb, and Cs, in the rhyolitic melt is accounted for by their lower activity in the acid melt. Among these elements, the small Li ion is characterized by a high z/r^2 ratio, which explains its preferential partition into more basic melt with a high NBO/T ratio.

Hence, we explain the uphill and downhill diffusion of alkalis and many trace elements by their "nonideality" in silicate melts. This nonideality determines the direction and gradient of their redistribution between coupled silicate melts, and their fast diffusion (enhanced by convection) ensures the efficiency of this mechanism.

IMPLICATIONS

Now it is generally agreed that magmas of various compositions experience temperature- and composition-driven convection. The uphill diffusion of alkalis from the basaltic to rhyolitic melts serves as an efficient

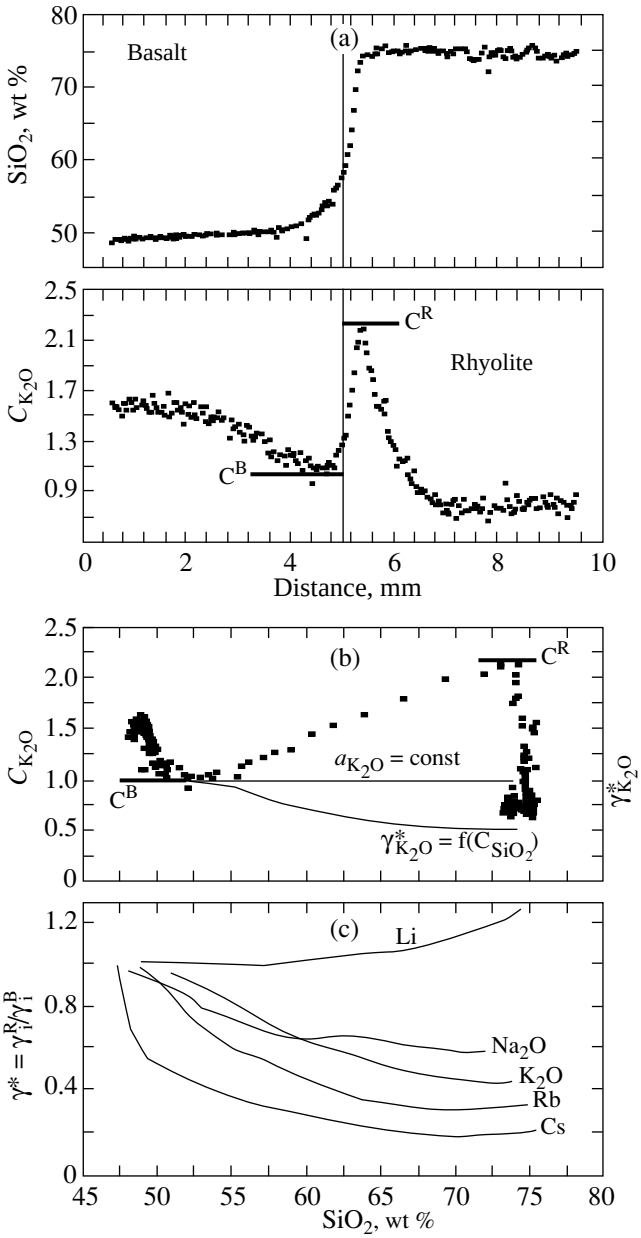

Fig. 4. Graphic representation illustrating the hypothesis of the constant activity of fast-diffusing K_2O between the peaks of its concentration (C_{K_2O}) at a coupled change in SiO_2 concentration (C_{SiO_2}).

(a) Variations in C_{K_2O} and C_{SiO_2} along the diffusion profile across the coupled melts.

(b) Variations in C_{K_2O} as a function of C_{SiO_2} (in compliance with the condition of constant activities between the peaks, the activity coefficient should be a function of the form $1/C_{K_2O}$.

(c) Activity coefficients (determined in a similar manner) of other alkaline trace elements between their concentration peaks (see Fig. 2) as functions of SiO_2. Note the more vigorous dependences of alkalis with larger ionic radii.

[1] The NBO/T ratio is the fraction of nonbridging oxygen in the melt.

mechanism that is able to stimulate and maintain composition-driven convection in each of the coupled melts. This convection sustains vigorous diffusion gradients at the interface between the two magmas and ensures the redistribution of fast-diffusing trace elements in accordance with their IKPC. Hence, convection sustains for a long time gradients of the activity coefficients of fast-diffusing trace elements. These gradients serve as a driving force of the redistribution of these elements between the magmas. It follows that the uphill diffusion of alkalis is, in our case, both the necessary condition of convection and the driving force of trace-element redistribution. At the same time, our experiments also demonstrate the important role of alkalis in composition-driven convection in more general cases. Since alkalis have the largest molar volumes and diffuse faster than most other major components, their uphill or downhill diffusion in long-living magmatic chambers is able to create local density variations and initiate composition-driven convection.

The direction of diffusion of alkalis depends on their initial concentrations in the coupled magmas. Downhill diffusion and convection in accordance with the mechanism described above require an alkali basaltic magma and a rhyolitic magma of normal alkalinity. In this sense, alkaline basaltic magma underplating the low- or normal-density continental crust (as, for example, Archean gray gneisses) and melting it can serve as a source of alkalis, which will redistribute into the newly formed acid melt in accordance with the uphill diffusion mechanism.

Fast-diffusing trace elements, except alkalis, redistribute from the rhyolitic to basaltic melt. This implies that, in the course of the long-lasting coexisting between a fresh basaltic melt portion, which replenished the magma chamber, and the rhyolite melt, the excess of fast-diffusing trace elements will be "buffered." This is particularly important for incompatible trace elements (such as Ba, La, and Ce), which enrich residual rhyolitic melts during their fractionation. As our experiments demonstrate, these elements will redistribute back into the basaltic melt. The redistribution of alkalis and many trace elements between melts proceeds in accordance with their IKPC (Fig. 3), which are different for distinct elements. This mechanism is able to modify petrologically important element ratios. Convection of any type (either temperature- or composition-driven) sustains strong chemical gradients, which serve as the driving force of trace-element diffusion and redistribution between magmas.

ACKNOWLEDGMENTS

The authors thank A.T. Anderson (University of Chicago), L.L. Perchuk, P.Yu. Plechov (Moscow State University), and F. Richter (University of Chicago) for useful comments. R.S. Newton, L.Ya. Aranovich, and I. Steel (University of Chicago) are thanked for help in the work at the experimental laboratory and with a microprobe.

REFERENCES

Baker, D.R., Estimation of Diffusion Coefficients during Interdiffusion of Geologic Melts: Application of Transition State Theory, *Chem. Geol*., 1992, vol. 98, pp. 11–21.

Bindeman, I.N. and Davis, A.M., Ion Microprobe Study of Basalt–Rhyolite Mixing Experiments: Convection, Uphill Diffusion, and Trace Element Exchange, *EOS Trans. Am. Geophys. Union*, 1997, vol. 78, p. 332.

Bindeman, I.N. and Perchuk, L.L., Experimental Studies of Magma Mixing at High Pressures, *Int. Geol. Rev.*, 1993, vol. 35, pp. 721–733.

Bindeman, I.N., Davis, A.M., and Drake, M.J., An Ion Microprobe Study of Plagioclase–Basalt Partition Experiments at Natural Concentration Levels of Trace Elements, *Geochim. Cosmochim. Acta*, 1998, vol. 62, no. 7, pp. 1175–1193.

Bottinga, Y. and Weill, D.F., The Viscosity of Magmatic Silicate Liquids: a Model for Calculation, *Am. J. Sci*., 1972, vol. 272, pp. 438–475.

Christensen, U., Instability of Hot Boundary Layer and Initiation of Thermo-Chemical Plumes, *Ann. Geophys.*, 1984, pp. 311–320.

Hofmann, A.W., Diffusion in Natural Silicate Melts: a Critical Review, *Physics of Magmatic Processes*, Hargraves, R.B., Ed., Princeton: Princeton Univ., 1980, pp. 315–417.

Holloway, J.R. and Blank, J.G., Application of Experimental Results to C–O–H Species in Natural Melts, *Rev. Mineral*., 1994, vol. 30, pp. 187–225.

Holloway, J.R., Pan, V., and Gudmundsson, G., High-Pressure Fluid-absent Melting Experiments in the Presence of Graphite: Oxygen Fugacity, Ferric/Ferrous Ratio and Dissolved CO_2, *Eur. J. Mineral*., 1992, vol. 4, pp. 105–114.

Huppert, H.E. and Sparks, R.S.J., The Generation of rhyolitic Magma by Intrusion of Basalt into Continental Crust, *J. Petrol*., 1988, vol. 29, pp. 599–624.

Jambon, A., Tracer Diffusion in rhyolitic Melts: Experimental Results for Na, K, Ca, Sr, Ba, Ce, Eu, to 1300°C and a Model of Calculation, *J. Geophys. Res*., 1982, vol. 87, pp. 10797–10810.

Korzhinskii, D.S., Acid–Basic Interaction of Components in Silicate Melts, in *Issledovanie natural'nogo i tekhnicheskogo mineraloobrazovaniya* (Studies in Natural and Technological Mineral Formation), Moscow: Nauka, 1966, pp. 5–9.

Kress, V.C. and Ghiorso, M.S., Multicomponent Diffusion in $MgO–Al_2O_3–SiO_2$ and $CaO–MgO–Al_2O_3–SiO_2$ Melts, *Geochim. Cosmochim. Acta*, 1993, vol. 57, pp. 4453–4466.

Kushiro, I., A New Furnace Assembly with a Small Temperature Gradient in Solid-Media, High-Pressure Apparatus, *J. Geophys. Res*., 1976, vol. 81, pp. 6347–6350.

LaTourrette, T., Wasserburg, G.J., and Fahey, A.J., Self Diffusion of Mg, Ca, Ba, Nd, Yb, Ti, Zr, and U in Haplobasaltic Melt, *Geochim. Cocmochim. Acta*, 1996, vol. 60, pp. 1329–1340.

Lange, R.L. and Carmichael, I.S.E., Thermodynamic Properties of Silicate Liquids with Emphasis on Density, Thermal Expansion and Compressibility, *Rev. Mineral*., 1990, vol. 24, pp. 25–64.

Lesher, C.E., Hervig, R.L., and Tinker, D., Self Diffusion of Network Formers Si and O in Naturally Occurring Basaltic Liquid, *Geochim. Cosmochim. Acta*, 1996, vol. 60, pp. 405–413.

Lesher, C.E., Kinetics of Sr and Nd Exchange in Silicate Liquids: Theory, Experiments, and Application to Uphill Diffusion, Isotopic Equilibration, and Irreversible Mixing of Magmas, *J. Geophys. Res*., 1994, vol. 99, pp. 9585–9604.

Liang, Y., Richter, F.M., Davis, A.M., and Watson, E.B., Diffusion in Silicate Melts: 1—Self Diffusion in the System $CaO–SiO_2–Al_2O_3$ at 1500°C and 1 Pa, *Geochim. Cosmochim. Acta*, 1996, vol. 60, pp. 1111–1113.

Litvinovsky, B.A. and Podladchikov, Y.Y., Crustal Anatexis during the Influx of Mantle Volatiles, *Lithos*, 1993, vol. 39, pp. 93–107.

MacPherson, G.J. and Davis, A.M., A Petrologic and Ion Microprobe Study of a Vigarano Type B Refractory Inclusion: Evolution by Multiple Stages of Alteration and Melting, *Geochim. Cosmochim. Acta*, 1993, vol. 57, pp. 231–243.

Marsh, B.D., On Convective Style, Vigour in Sheet-like Magmatic Chambers, *J. Petrol*., 1989, vol. 30, pp. 479–530.

Minarik, W.G., Ryerson, F.J., Hutcheon, I.D., and McKeegan, K.D., More Immiscible Silicate Melt Partitioning: Light Lithophile and Platinum Group Elements, *EOS Trans. Am. Geophys. Union*, 1996, vol. 77, p. 841.

Mysen, B.O., Relations Between Structure, Redox Equilibria of Iron, and Properties of Magmatic Liquids, *Advances in Physical Geochemistry*, Perchuk, L.L. and Kushiro, I., Eds., New York: Springer, 1991, vol. 6, pp. 120–151.

Perez, W.A. and Dunn, T., Diffusivity of Sr, Nd, and Pb in Natural Rhyolite at 1GPa, *Geochim. Cosmochim. Acta*, 1996, vol. 60, pp. 1387–1397.

Richter, F.M., A Method for Determining Activity–Composition Relations Using Chemical Diffusion in Silicate Melts, *Geochim. Cosmochim. Acta*, 1993, vol. 57, pp. 2019–2032.

Ryerson, F.J. and Hess, P.C., Implications of Liquid–Liquid Distribution Coefficients to Mineral–Liquid Partitioning, *Geochim. Cosmochim. Acta*, 1978, vol. 42, pp. 921–932.

Thompson, R.N. and Kushiro, I., The Oxygen Fugacity Within Graphite Capsules in Piston–Cylinder Apparatus at High Pressures, *Carnegie Inst. Washington, Year Book*, 1972, vol. 71, pp. 615–616.

Vicenzi, E., Green, T., and Sie, S., Effect of Oxygen Fugacity on Trace Element Partitioning Between Immiscible Liquids at Atmospheric Pressure, *Chem. Geol*., 1994, vol. 117, pp. 355–360.

Watson, E.B. and Baker, D.R., Chemical Diffusion in Magmas: An Overview of Experimental Results and Geochemical Applications, *Advances in Physical Geochemistry*, Perchuk, L.L. and Kushiro, I., Eds., New York: Springer, 1991, vol. 6, pp. 120–151.

Watson, E.B., Two-Liquid Partition Coefficients: Experimental Data and Geochemical Implications, *Contrib. Mineral. Petrol*., 1976, vol. 56, pp. 119–134.

Wiebe, R.A., Mafic–Silicic Layered Intrusions, *Geol. Soc. Am. Spec. Publ*., 1996, vol. 315, pp. 233–242.

Zhang, Y., A Modified Effective Binary Diffusion Model, *J. Geophys. Res*., 1993, vol. 98, pp. 11901–11920.